

Oxygen isotope fractionation between gypsum and its formation waters: implications for past chemistry of the Kawah Ijen volcanic lake, Indonesia.

Sri Budhi Utami^{1*}°, Vincent J. van Hinsberg¹, Bassam Ghaleb², Arnold E. van Dijk³

1. Department of Earth and Planetary Sciences
McGill University
3450 University Street
Montreal, QC, Canada H3A 0E8
Email: V.J.vanHinsberg@gmx.net

2. GEOTOP
Université du Québec à Montréal
C.P. 8888, Succ. Centre-Ville
Montréal, QC, Canada H3C 3P8
Email: ghaleb.bassam@uqam.ca

3. Faculty of Geosciences
Utrecht University
Princetonlaan 8
3584 CB Utrecht
the Netherlands
Email: A.E.vanDijk@uu.nl

*Corresponding author

° Current address:
Asian School of the Environment
Nanyang Technological University
50 Nanyang Avenue, N2-01A-15
Singapore 639798

Email: sri.budhi.utami@gmail.com

Abstract

1 Gypsum ($\text{CaSO}_4 \cdot 2\text{H}_2\text{O}$) provides an opportunity to obtain information from both the oxygen
2 isotopic composition of the water and sulfate of its formation waters, where these components
3 are commonly sourced from different reservoirs (e.g. meteoric vs. magmatic). Here, we present
4 $\delta^{18}\text{O}$ values for gypsum and parent spring waters fed by the Kawah Ijen crater lake in East Java,
5 Indonesia, and from these natural samples derive gypsum-fluid oxygen isotope fractionation
6 factors for water and sulfate group ions of $1.0027 \pm 0.0003\text{‰}$ and $0.999 \pm 0.001\text{‰}$, respectively.
7 Applying these fractionation factors to a growth-zoned gypsum stalactite that records formation
8 waters from 1980 to 2008 during a period of passive degassing, and gypsum cement extracted
9 from the 1817 eruption tephra fall deposit, shows that these fluids were in water-sulfate oxygen
10 isotopic equilibrium. However, the 1817 fluid was $>5\text{‰}$ lighter. This indicates that the 1817 pre-
11 eruption lake was markedly different, and had either persisted for a much shorter duration or was
12 more directly connected to the underlying magmatic-hydrothermal system. This exploratory
13 study highlights the potential of gypsum to provide a historical record of both the $\delta^{18}\text{O}_{\text{water}}$ and
14 $\delta^{18}\text{O}_{\text{sulfate}}$ of its parental waters, and to provide insights into the processes acting on volcanic
15 crater lakes or any other environment that precipitates gypsum.

Keywords: gypsum, oxygen isotopes, crystalline water, sulfate group, isotope fractionation
factor, Kawah Ijen, volcanic lake

16 **Introduction**

17

18 Sulfate minerals are common in volcanic systems, both as primary accessory minerals and
19 secondary minerals associated with magmatic-hydrothermal fluids and sulfate in aerosols from
20 SO₂ oxidation in the volcanic plume (Mather et al., 2006). The sulfate mineralogy is varied and
21 includes alunite-jarosite, barite, gypsum, anhydrite, alum and leonite. Calcium sulfates (gypsum
22 and anhydrite) are particularly common, and are found as a primary igneous mineral in the
23 eruption products of volcanoes including El Chichon and Redoubt (Luhr et al., 1984; Rye et al.,
24 1984; Luhr, 2008; Swanson and Kearney, 2008), as mineral encrustations or sublimate minerals
25 around fumaroles (Africano and Bernard, 2000), as precipitates from acidic waters where
26 volcanoes host crater lakes or acid streams (e.g. Delmelle and Bernard, 1994; Takano et al.,
27 2004; Inguaggiato et al., 2018), and in subsurface alteration products (Fulignati et al., 1998).
28 Hence, sulfates from volcanic environments have the potential to provide information on a
29 multitude of volcanic processes.

30

31 In an earlier study (Utami et al., 2019), we have explored the potential of growth-zoned gypsum
32 precipitated from crater lake effluent to provide a record of volcanic activity from a gypsum
33 stalactite and gypsum cementing the base tephra fall deposit from the 1817 phreato-magmatic
34 eruption, as determined from its trace elemental compositions. We showed the presence of a
35 compositional signal that correlates with the degree of activity at the Kawah Ijen crater lake in
36 Indonesia. Here, we investigate the potential of the complementary record provided by stable
37 isotopes, specifically the ¹⁸O/¹⁶O oxygen isotope ratio. In particular, oxygen occurs in two
38 different sites within the crystalline structure of gypsum; in structurally bound water, and in the
39 sulfate group. Gypsum therefore samples two oxygen reservoirs from its formation waters; H₂O
40 and SO₄ which commonly have different sources. Whereas H₂O is sourced from rain,

Manuscript – Revision 1

41 groundwater and the magmatic-hydrothermal system, SO₄ comes from volcanic gases and the
42 subsequent disproportionation reactions to produce sulfate group ions (Kusakabe et al., 2000;
43 Delmelle and Bernard 2015). In highly concentrated brines such as those found in the Kawah
44 Ijen and Poás crater lakes, sulfate contains in excess of 5% by mass of oxygen (cf. Delmelle and
45 Bernard, 1994; Martínez et al., 2000). Isotopic equilibration between these oxygen reservoirs is
46 sluggish (Hoering and Kennedy, 1957; Chiba and Sakai, 1985, van Stempvoort and Krouse,
47 1994), which potentially allows for preservation of original oxygen isotopic signatures, as well
48 as their use in geothermometry (see Seal et al., 2000). For minerals incorporating both water and
49 sulfate and with slow intra-mineral oxygen isotopic exchange, such a signature and its
50 differentiation between the two reservoirs would be preserved.

51

52 In this study we determined the oxygen isotopic fractionation factors between gypsum and its
53 hyperacidic formation waters for both the crystalline water and sulfate group oxygen. We apply
54 these data to a growth zoned gypsum stalactite precipitated over a >40 year period from seepage
55 waters of the Kawah Ijen crater lake in Indonesia and gypsum associated with its 1817 phreato-
56 magmatic eruption to explore whether the oxygen isotopic record can help us understand Kawah
57 Ijen's past volcanic activity. This study forms part of a broader effort to explore the use of
58 elemental and isotopic compositions of growth-zoned gypsum to provide information on the
59 timing, types and characteristics of past volcanic activity of the Kawah Ijen system.

60

61 **Geological setting**

62

63 Ijen volcano in East Java, Indonesia, is a passively degassing basaltic to dacitic stratocone
64 (Kemmerling, 1921; Delmelle and Bernard, 1994; Handley et al., 2007; van Hinsberg et al.,

Manuscript – Revision 1

65 2010, 2017) capped by the Kawah Ijen volcanic lake, the world's largest hyper-acidic crater lake
66 (Figure 1). Historical records indicate that there has been a crater lake since at least the 19th
67 century (Lechenault de la Tour, 1805, "Oudgast", 1820). Currently, the lake contains $2.8 \times 10^7 \text{m}^3$
68 of pH 0-0.1 sulfate-chloride-rich brine with a total dissolved solute content of $\sim 100 \text{mg/kg}$
69 (Delmelle and Bernard, 1994; Takano et al., 2004; Caudron et al., 2015). The lake temperature is
70 around 40°C , although surface temperature is commonly lower due to cooling by wind or rain
71 (Lewicki et al., 2017). The extreme composition and high elemental load derives from the flux of
72 volcanic gases into the lake and interaction between lake water and wall rocks (Delmelle and
73 Bernard, 1994; Delmelle et al., 2000; van Hinsberg et al., 2010; 2017). The lake water seeps
74 through the volcanic edifice and emerges in several springs on the western flank, forming the
75 headwaters of the acidic Banyu Pahit river (Figure 1). Gypsum precipitates abundantly around
76 these springs as a result of cooling and evaporation of the water and is present as cm-sized
77 stalactites, efflorescences, and, at the uppermost springs, as an up to 30cm thick plateau (Utami
78 et al, 2019). The stalactites and plateau gypsum display growth zoning, locally interrupted by
79 sediment layers. Gypsum precipitation is a long-lived feature of the Kawah Ijen system and was
80 already reported at the plateau site for a visit in 1796 ("Oudgast", 1820).

81

82 Ijen volcano poses significant volcanogenic hazards to communities living within the Ijen
83 caldera, the Asambagus plain, and the nearby city of Banyuwangi, related to both volcanic
84 activity and the metal-laden acidic effluent of the Banyu Pahit river. The most recent eruption
85 occurred in 1817, which was a phreato-magmatic event that expelled the pre-existing lake,
86 deepened and enlarged the crater, and led to the deposition of extensive phreatic to phreato-
87 magmatic fall and lahars deposits (Junghuhn, 1853; Bosch, 1858; Caudron et al., 2015). Since

88 then, volcanic unrest at Kawah Ijen is dominated by phreatic and steam explosions, and gas
89 emissions (Caudron et al., 2015, 2017). Only a comparatively scant historical record of its
90 volcanic activity exists, which has led to recent efforts to improve both the active monitoring and
91 reconstruction of its volcanic past (Gunawan et al., 2017).

92

93 **Methodology**

94 A concentric growth-zoned gypsum stalactite was sampled in 2009 from the gypsum plateau
95 at the seepage springs closest to the lake (Figure 1). At the time of the sampling, the gypsum
96 stalactite was actively growing and representative of the typical stalactites found in the area. The
97 stalactite measured 12cm in length with a 5cm base diameter. Transparent gypsum laths that
98 form the actively growing tips were also sampled from multiple stalactites. The sampled tips
99 represent one year of growth, as the tips were removed from these specific stalactites in 2008.
100 The large stalactite is covered in mm-sized idiomorphic gypsum laths growing outward in all
101 directions and also displays internal concentric growth zoning (see Fig. 3c of Utami et al.,
102 2019). The stalactite is dense and growth appears to be restricted to its outer surface, where new
103 gypsum laths grew on older laths that served as substrates. The tips consist of up to 5cm long, 4
104 mm wide idiomorphic transparent laths of gypsum, commonly twinned (Fig 3b. of Utami et al.,
105 2019).

106

107 Gypsum cementing the base tephra fall deposit from the 1817 phreato-magmatic eruption was
108 sampled in a separate field campaign in 2014. The tephra fall deposit consists of well-sorted,
109 mm-sized, grain-supported, variably altered tephra fragments cemented by transparent needles of
110 gypsum (Fig 3e of Utami et al., 2019). The gypsum needles are interpreted as precipitates from

111 an interstitial lake-derived fluid that was incorporated in the fall material during the initial lake
112 expelling phreatic eruption. The tephra fall horizon is further covered by 7 to 8 m of phreatic to
113 magmatic deposits from the later phases of the 1817 eruption, including cm-thick impermeable
114 lahars layers.

115

116 The gypsum stalactite tips and gypsum laths from the tephra fall were crushed and transparent
117 fragments clear of inclusions handpicked using a binocular microscope. The larger stalactite was
118 sectioned perpendicular to its long axis and 3 growth zones representing core, mantle and rim
119 were sampled in-situ using a small diamond rotary saw. These samples came from between the
120 zones used by Utami et al. (2019) to date the stalactite. The sampled material was crushed,
121 washed with distilled water, and further checked for inclusions under a binocular microscope
122 prior to further analyses. The gypsum separates were then ground to a fine powder in an agate
123 mortar under ethanol and dried in a desiccator. Elemental compositions for the stalactite and
124 gypsum cement were presented in Utami et al. (2019). The seepage water from which these
125 stalactites grow was also sampled. The water sample was filtered in the field through a 0.45 μm
126 disposable filter and stored in cleaned HDPE bottles, free of air.

127

128 **$\delta^{18}\text{O}$ analyses of the fluid sample.** Sulfate in the spring water (sample KV15-006) was
129 precipitated as BaSO_4 by adding an excess of dried BaCl_2 after a two-fold dilution with nano-
130 pure water. This dilution was to convert HSO_4^- ions to SO_4^{2-} prior to the precipitation reaction
131 and hence ensure a complete transfer of dissolved SO_4 to solid BaSO_4 as motivated by
132 thermodynamic modeling using PHREEQC 2.17 and the Lawrence Livermore National
133 Laboratory database (Parkhurst and Appelo, 1999). The barite and the residual fluid, as well as

134 the nano-pure water used to dilute the fluid were analyzed for their $\delta^{18}\text{O}$ at the Environmental
135 Isotope Laboratory at the University of Waterloo. For further details on the barite analyses to
136 obtain $\delta^{18}\text{O}_{\text{fluidSO}_4}$, see below. The $\delta^{18}\text{O}_{\text{fluidH}_2\text{O}}$ was determined by equilibration of the
137 fluid samples with an injected volume of CO_2 , followed by isotope ratio mass spectrometry
138 (IRMS).

139

140 **$\delta^{18}\text{O}$ analyses of oxygen in gypsum crystalline water.** Thermogravimetric analysis of
141 a Kawah Ijen gypsum sample showed loss of crystalline water in two distinct steps centred at
142 150 and 180°C (for a 10°C/min heating rate). Dehydration was completed at *ca.* 300°C with
143 100% of the theoretical mass loss. Further mass changes were observed above 600°C. There was
144 no evidence for any absorbed water in the dried gypsum powder, nor of loss of crystalline water.
145 The crystalline water for the isotope analyses was extracted from the dried gypsum powders by
146 heating to 400°C and the water subsequently captured in a cold-trap. The water was then
147 equilibrated with an injected volume of CO_2 and measured by IRMS (Thermo GasBench-II
148 coupled to a Thermo Delta-V) in the stable isotope laboratory of Utrecht University. The small
149 gypsum sample amounts provided only *ca.* 50 μL of water, and a correction had to be developed
150 to account for differences in the fraction of water evaporating into the headspace (relatively more
151 for smaller samples) and the resulting isotope fractionation. This correction was determined by
152 measuring variable amounts (30 to 150 μL) of in-house standards (RMW - distilled water, K –
153 Kottasberggen, Greenland snow, and RSW - distilled seawater) and found to be systematic and
154 predicatable (supplementary Figure S1), with a stronger deviation the smaller the water volume
155 and the lower the $\delta^{18}\text{O}$ of the standard (the latter is related to the positive $\delta^{18}\text{O}$ of the CO_2 , which
156 is +0.32‰). The correction required for the gypsum crystalline water samples was minimal
157 (supplementary Figure S1).

158
159 **$\delta^{18}\text{O}$ analyses of oxygen in the sulfate group of gypsum.** The gypsum powders were
160 dissolved overnight in nano-pure water in the presence of a small amount of dissolved HgCl_2 to
161 extract any sulfide, which was filtered out. The dissolved SO_4^{2-} ions in the resulting filtrate were
162 precipitated as BaSO_4 by adding 99.9% pure $\text{BaCl}_2 \cdot \text{H}_2\text{O}$ powder in excess (1g of $\text{BaCl}_2 \cdot \text{H}_2\text{O}$ for
163 50 mg of gypsum). The BaSO_4 powder was collected by filtration, washed with nano-pure water
164 and dried overnight at 60-70°C in a convection oven. The BaSO_4 powder was analysed for $\delta^{18}\text{O}$
165 at the Environmental Isotope Laboratory at the University of Waterloo by pyrolysis at 1450°C
166 using an Elementar Pyrocube elemental analyzer coupled to an IsoPrime Continuous Flow
167 IRMS.

168 **Results**

169 The $\delta^{18}\text{O}_{\text{gypsum}}^{\text{H}_2\text{O}}$ and $\delta^{18}\text{O}_{\text{gypsum}}^{\text{SO}_4}$ of gypsum vary between 4.3 - 9.8‰ and 16.8 - 23.1‰,
170 respectively, whereas the corresponding values for the fluid sample are 6.9 and 23.3‰ (all
171 values relative to V-SMOW/V-SLAP - Table 1). The accuracy of analyses is between 0.2 and
172 0.5‰ (1 standard deviation) for $\delta^{18}\text{O}_{\text{water}}$ and 0.3 to 0.4‰ (1s) for $\delta^{18}\text{O}_{\text{sulfate}}$ as determined on a
173 range of certified international and cross-calibrated in-house reference materials. The precision,
174 as determined from replicate analyses is 0.1, 0.3 and 0.3, 0.1 (1s) for $\delta^{18}\text{O}_{\text{water}}$ and $\delta^{18}\text{O}_{\text{sulfate}}$ for
175 solids and fluids, respectively (Table 1). Sufficient material was available for the stalactite tip
176 sample (KV09-505) to be measured at variable sample amounts. Results are identical within
177 error after correction for extracted water amounts of 48, 55, 62 and 152 μL (Table 1). The
178 $\delta^{18}\text{O}_{\text{fluid}}^{\text{H}_2\text{O}}$ and $\delta^{18}\text{O}_{\text{fluid}}^{\text{SO}_4}$ values are similar to those reported by Delmelle and Bernard (2000) for
179 the seepage area spring waters. The $\delta^{18}\text{O}_{\text{fluid}}^{\text{H}_2\text{O}}$ is within the range reported by these authors ($6.9 \pm$
180 0.3‰ compared to 2 to 7.8‰), whereas the $\delta^{18}\text{O}_{\text{fluid}}^{\text{SO}_4}$ is about 1‰ higher. The $\delta^{18}\text{O}_{\text{gypsum}}^{\text{H}_2\text{O}}$ for

181 the gypsum tip and stalactite samples is similar, whereas the gypsum cement is 5.5‰ lighter. The
182 gypsum $\delta^{18}\text{O}_{\text{gypsum}}^{\text{SO}_4}$ values are more variable, with the stalactite around 2‰ heavier and the
183 cement 3.8‰ lighter, compared to the gypsum tips (Table 1).

184

185 Discussion

186 The $\delta^{18}\text{O}_{\text{fluid}}^{\text{H}_2\text{O}}$ and $\delta^{18}\text{O}_{\text{fluid}}^{\text{SO}_4}$ of Ijen seepage waters are high when compared to local meteoric
187 water ($\delta^{18}\text{O}_{\text{meteoric}}^{\text{H}_2\text{O}} = -9\text{‰}$, Delmelle et al., 2000; Palmer, 2009), Kawah Ijen fumaroles
188 ($\delta^{18}\text{O}_{\text{fumaroles}}^{\text{H}_2\text{O}} = 3.6\text{‰}$ and $\delta^{18}\text{O}_{\text{fumaroles}}^{\text{SO}_4} = 7.6\text{‰}$, van Hinsberg et al., 2017), or seawater
189 ($\delta^{18}\text{O}_{\text{seawater}}^{\text{H}_2\text{O}} = 0.2\text{‰}$ and $\delta^{18}\text{O}_{\text{seawater}}^{\text{SO}_4} = 9.3\text{‰}$, Lloyd, 1967; Schmidt, 1999). Dissolved sulfate
190 in acidic crater lakes dominantly derives from disproportionation reactions that convert volcanic
191 SO_2 to $\text{SO}_4^{2-}(\text{aq})$ via various intermediaries, with H_2S oxidation being a negligible contributor
192 (Kusakabe et al., 2000; Delmelle and Bernard 2015). This process is likely entirely abiotic given
193 that no sulfur-oxidizing organisms were detected in the Ijen lake or most-acidic Banyu Pahit
194 river water samples by Löhner et al. (2006). The heavy $\delta^{18}\text{O}_{\text{fluid}}^{\text{SO}_4}$ is therefore a direct reflection of
195 abiotic SO_2 disproportionation, and conversion of SO_2 to dissolved sulfate can indeed lead to an
196 up to 31‰ enrichment in ^{18}O (Müller et al., 2013a,b). The heavy $\delta^{18}\text{O}_{\text{fluid}}^{\text{H}_2\text{O}}$ compared to local
197 meteoric water has been explained by strong evaporative enrichment of the lake water combined
198 with input of heavy water from the magmatic-hydrothermal system (Delmelle et al., 2000).

199

200 **Equilibrium in water-sulfate $\delta^{18}\text{O}$.** The $\delta^{18}\text{O}_{\text{fluid}}^{\text{H}_2\text{O}}$ and $\delta^{18}\text{O}_{\text{fluid}}^{\text{SO}_4}$ are close to isotopic
201 equilibrium when compared to the sulfate-water fractionation curve of Zeebe (2010) at the $\sim 40^\circ\text{C}$
202 temperature of the springs (Table 2). Oxygen isotopic disequilibrium has been reported for the

203 lake water and fumarole emissions at Kawah Ijen (Delmelle et al., 2000; van Hinsberg et al.,
204 2017), although the lake disequilibrium is less pronounced when the fractionation factors of
205 Zeebe (2010) are used. This disequilibrium could indicate preservation of a previous, higher
206 temperature oxygen exchange equilibrium state (see Delmelle et al., 2000). However, the
207 dominant sources of water and sulfate to the lake differ, with the latter derived from the
208 magmatic-hydrothermal system, whereas the former has a strong meteoric contribution
209 (Delmelle et al., 2000; van Hinsberg et al., 2017). The disequilibrium could thus also reflect
210 incomplete re-equilibration between these sources. Even at a pH of zero, the isotopic exchange
211 half-life is approximately 11 years at a water temperature of 40°C (Fig. 12 of Seal et al., 2000).
212 Zeebe (2010) shows a strong difference in oxygen isotope fractionation between HSO_4^- - H_2O and
213 SO_4^{2-} - H_2O and it would seem reasonable to assume that a further difference develops when a
214 significant fraction of sulfate is present as complexes with cations, as is the case for Ijen volcanic
215 lake waters based on thermodynamic speciation modeling. Isotopic equilibrium would be
216 expected for the lake given the lack of any isotopic variation with depth (Delmelle et al., 2000)
217 and the expected long residence time of water and sulfate in the large lake volume (see also
218 below for a discussion of residence times).

219

220 Gypsum precipitates from the seepage waters by evaporation and cooling of the fluid with an
221 average stalactite growth rate of 340 $\mu\text{m}/\text{year}$ (Utami et al., 2019). Partitioning of trace elements
222 between gypsum and its parent fluid is predictable and obeys Lattice-Strain theory (van Hinsberg
223 and Williams-Jones 2008). This slow growth rate and systematic element partitioning suggests
224 formation at equilibrium conditions, and we assume that this is also the case for its oxygen
225 isotopic composition, although we acknowledge that we lack direct evidence for this. There are

226 no data on the kinetics of O-isotopic equilibration between H₂O and SO₄ within gypsum.
227 However, experiments suggest it to be slow (Gonfiantini and Fontes, 1963). We therefore
228 conclude that gypsum would preserve the isotopic composition captured from the fluid over the
229 timescales reported here.

230

231 **Oxygen fractionation between fluid and gypsum.** Gypsum-fluid oxygen-isotope
232 fractionation factors for crystalline water and the sulfate group (Figure 2) were calculated from
233 the gypsum tip sample and its corresponding brine, as well as by combining the stalactite D
234 growth zone with the 2009 brine, and the B-C growth zone with the seepage fluid composition
235 reported by Delmelle and Bernard (2000). The latter two do not represent a direct equilibrium
236 pair and are offset in time (growth zones D and B-C formed in 2008 and 1991, respectively
237 (Utami et al., 2019), and the data from Delmelle and Bernard (2000) are for 1996 seepage water).
238 Nonetheless, the fractionation factors from these three sets are similar (Table 2). Gypsum
239 preferentially incorporates ¹⁸O in its crystalline water, but ¹⁶O for the sulfate group, with mean
240 gypsum-water fractionation factors of 1.0027 ± 0.0002 and 0.9990 ± 0.0014 , respectively
241 (uncertainties given as 1 standard deviation). The set consisting of zone B-C with the Delmelle
242 and Bernard (2000) seepage fluid gives a fractionation factor of 1.0005 for sulfate. This is the set
243 for which equilibrium is least constrained and with $\delta^{18}\text{O}_{\text{sulfate}}$ from two different labs, and we are
244 therefore more confident in the fractionation factors from the other two sets. Nevertheless, it is
245 clear from these data that the oxygen isotope fractionation between water and gypsum sulfate
246 group is small.

247

248 Earlier studies similarly found gypsum crystalline water to be heavy compared to its parent
249 solution in experiments, although their fractionation factors are higher at 1.0035 to 1.0041 with a
250 preferred value of 1.0035 ± 0.0002 (1s uncertainty, see Gazquez et al., 2017 for an overview).
251 This difference could reflect a difference in solution pH, given that the earlier studies were at
252 much higher, commonly circum-neutral pH, whereas the Kawah Ijen fluids have a pH of around
253 zero. Oxygen isotope fractionation is also known to depend on speciation and species hydration
254 (Truesdell, 1974; Horita et al., 1994), which is in turn strongly affected by pH. Unfortunately,
255 this has yet to be quantified for acidic SO_4 -rich solutions (cf. Stoffregen et al., 1994; Rouwet and
256 Ohba, 2015). Thus, published fractionation factors between the sulfate group and water may not
257 be directly applicable to volcanic brines like that of Ijen, in which case the observed $\alpha(\text{SO}_4$ -
258 $\text{H}_2\text{O})_{\text{fluid}}$ could represent the equilibrium fractionation factor at these acidic conditions. No
259 previous data are available on gypsum-water oxygen fractionation for sulfate group ions, but a
260 similar, differing fractionation behaviour for sulfate group and hydroxyl groups has been
261 reported for alunite and jarosite (Stoffregen et al., 1994; Rye and Stoffregen, 1995).

262

263 **Oxygen isotopic composition of stalactite and gypsum cement formation waters.** The
264 gypsum-water fractionation factors allow for the $\delta^{18}\text{O}_{\text{fluid}}^{\text{H}_2\text{O}}$ and $\delta^{18}\text{O}_{\text{fluid}}^{\text{SO}_4}$ of the parent fluids to be
265 calculated from gypsum (Figure 2). The $\delta^{18}\text{O}_{\text{fluid}}^{\text{H}_2\text{O}}$ compositions calculated from the growth-
266 zoned stalactite vary from $\delta^{18}\text{O} = 6.2$ to 7.1% , similar to the 6.9% of the present-day seepage
267 waters. The $\delta^{18}\text{O}_{\text{fluid}}^{\text{SO}_4}$ varies from 23.3 to 24.0% , which is somewhat heavier than the crystalline
268 water (Figure 3). In contrast, the gypsum cement formed from a fluid with significantly lighter
269 $\delta^{18}\text{O}$ for both H_2O and SO_4 at 1.6 and 18.1% , respectively. Despite these variations, the
270 fractionation factor between $\delta^{18}\text{O}$ for H_2O and SO_4 in the fluid is near constant (Table 3). The

271 consistency in $\alpha(\text{SO}_4\text{-H}_2\text{O})_{\text{fluid}}$, despite strong variations in $\delta^{18}\text{O}_{\text{fluid}}^{\text{H}_2\text{O}}$ and $\delta^{18}\text{O}_{\text{fluid}}^{\text{SO}_4}$, is
272 inconsistent with this representing incomplete re-equilibration; it is highly unlikely that the exact
273 same degree of temperature re-equilibration, or mixing of sources would be attained. This is
274 especially true for the 1817 gypsum cement, which samples a previous, smaller crater lake
275 (Caudron et al., 2015; Utami et al., 2019). We therefore conclude that this $\alpha(\text{SO}_4\text{-H}_2\text{O})_{\text{fluid}}$ more
276 likely reflects oxygen exchange equilibrium for these acidic brines, with the difference from the
277 theoretical $\alpha(\text{SO}_4\text{-H}_2\text{O})_{\text{fluid}}$ (Zeebe, 2010) reflecting the effects of pH and speciation on
278 fractionation.

279

280 **Historical $\delta^{18}\text{O}$ record from gypsum.** The historical record of seepage water $\delta^{18}\text{O}_{\text{fluid}}^{\text{H}_2\text{O}}$
281 and $\delta^{18}\text{O}_{\text{fluid}}^{\text{SO}_4}$ as based on direct fluid measurements and reconstructions from the gypsum
282 stalactite and 1817 gypsum cement is shown in Figure 4. The elemental record shows a distinct
283 change in behavior of the system around 1992, which marks the transition from quiescence to a
284 state of variable unrest (Caudron et al., 2015; Utami et al., 2019). The $\delta^{18}\text{O}$ record unfortunately
285 lacks the resolution needed to directly link the elemental and isotopic records together. The two
286 older samples that represent the period of quiescence are both lower in $\delta^{18}\text{O}_{\text{fluid}}^{\text{H}_2\text{O}}$ and higher in
287 $\delta^{18}\text{O}_{\text{fluid}}^{\text{SO}_4}$ compared to the more recent samples, but the differences are small and could represent
288 incremental variations in the lake chemistry over time. An important parameter in interpreting
289 the historical record is the residence time of water and sulfate in the lake, as this controls how
290 quickly changes will become apparent in the lake, and in the gypsum precipitating from it. To
291 estimate residence time, we use the approach of Rouwet and Tassi (2011), with elemental and
292 isotopic compositions for rain- and groundwater, volcanic gas, lake and seepage water, as well as
293 seepage flux, from van Hinsberg et al. (2017). The volcanic gas flux was estimated from the

294 change in Cl content of the lake over time and the Cl content of the volcanic gas, assuming that
295 the surface gas composition is identical to that of the gas entering the bottom of the lake. No loss
296 of Cl by evaporation was included in this calculation, and this is therefore a minimum estimate
297 (see Rodríguez et al. 2018). Annual precipitation for Kawah Ijen was taken from Blaak (1920),
298 which represents data for 1907-1917 (the annual precipitation for Banyuwangi reported by Blaak
299 (1920) is equivalent to that at present). Lake volume was taken from Caudron et al. (2015),
300 converted to mass using a density of 1.035 kg/dm³ as calculated from lake water composition. A
301 water residence time of 1.5 years results. Although this value has a large uncertainty given the
302 assumptions and uncertainties in the input parameters, it does indicate that gypsum would be
303 able to record changes on the multi-year timescale that we have reconstructed here.

304

305 In contrast to the small variations from 1980 to 2009, the 1817 sample is distinctly
306 different (Figure 4). This gypsum records the composition of crater lake waters thrown out
307 during the 1817 phreato-magmatic eruption of Kawah Ijen (Utami et al., 2019). Both the
308 $\delta^{18}\text{O}_{\text{water}}$ and $\delta^{18}\text{O}_{\text{sulfate}}$ of the 1817 gypsum cement are lighter than the gypsum stalactite and the
309 present-day gypsum stalactite tips. Whereas the stalactite grows in an open-system, continuously
310 refreshed fluid environment, the gypsum cement would likely have formed from a closed-system
311 pore fluid, resulting in ¹⁸O/¹⁶O isotope fractionation as gypsum precipitation progresses.
312 However, the above and below 1 fractionation factors for water and sulfate group, respectively,
313 would lead to diverging $\delta^{18}\text{O}_{\text{gypsum}}^{\text{H}_2\text{O}}$ and $\delta^{18}\text{O}_{\text{gypsum}}^{\text{SO}_4}$ in this case, whereas both are found to be
314 isotopically lighter. Secondary processes such as later water ingress and re-equilibration,
315 leaching of oxygen from the fall deposit rock clasts, or boiling of the fluid in the hot fall deposit
316 would almost exclusively modify $\delta^{18}\text{O}_{\text{gypsum}}^{\text{H}_2\text{O}}$ and thus introduce disequilibrium, whereas the

317 $\alpha(\text{SO}_4\text{-H}_2\text{O})_{\text{fluid}}$ appears to be at low-temperature equilibrium (Table 3). This argument also rules
318 out a significant meteoric water contribution added in the eruption plume. Thus we conclude that
319 the observed signature reflects a fluid with a different $\delta^{18}\text{O}_{\text{fluid}}^{\text{H}_2\text{O}}$ and $\delta^{18}\text{O}_{\text{fluid}}^{\text{SO}_4}$ signature. Given
320 that the $\alpha(\text{SO}_4\text{-H}_2\text{O})_{\text{fluid}}$ appears to be in equilibrium (Table 3), and the fact that the amount of
321 oxygen in sulfate is still subordinate to that in water in the Kawah Ijen fluids, we attribute the
322 low $\delta^{18}\text{O}_{\text{fluid}}^{\text{SO}_4}$ to disproportionation into, and equilibrating with a light $\delta^{18}\text{O}_{\text{fluid}}^{\text{H}_2\text{O}}$ reservoir. A
323 stronger fumarole contribution cannot be excluded, but this would need to be significantly larger,
324 and is not able to explain the $\delta^{18}\text{O}_{\text{fluid}}^{\text{H}_2\text{O}}$ that extends below the oxygen isotopic composition of the
325 fumaroles (Figure 4). Volatile metal ratios suggest a stronger contribution from deep, basaltic
326 magma prior to the 1817 eruption (Utami et al., 2019), but it is unclear how this would affect the
327 $\delta^{18}\text{O}$ signature. Addition of meteoric water would lower the $\delta^{18}\text{O}_{\text{fluid}}^{\text{H}_2\text{O}}$ given its $\delta^{18}\text{O}$ of around -
328 9‰ (Delmelle et al., 2000; Palmer, 2009). Water-rock interaction would also lower the $\delta^{18}\text{O}$ of
329 the fluid as ^{18}O gets enriched in the altered amorphous silica residue. However, there is no
330 evidence that the pre-eruptive lake was more dilute or more concentrated than at present (van
331 Hinsberg et al., 2017). Delmelle et al. (2000) show that the high $\delta^{18}\text{O}_{\text{fluid}}^{\text{H}_2\text{O}}$ of the current lake
332 requires significant evaporative loss of ^{16}O . This evaporation gradually increases the $\delta^{18}\text{O}$ of the
333 lake, and the lower $\delta^{18}\text{O}$ of the pre-eruptive lake may therefore indicate that it had been present
334 for a shorter duration. Less evaporation because of a lower fluid temperature can be ruled out,
335 because this would be reflected in the $\alpha(\text{SO}_4\text{-H}_2\text{O})_{\text{fluid}}$. The lake had a smaller surface area prior
336 to the 1817 eruption (Leschenault de la Tour 1805; Caudron et al. 2015), whereas the crater itself
337 was similar in size, which would suggest a larger rain- and groundwater flux relative to
338 evaporation, compared to the present-day. Alternatively, the pre-1817 lake had a more direct
339 connection to the magmatic-hydrothermal system, and therefore a stronger contribution of

340 $\delta^{18}\text{O}_{\text{fluid}}^{\text{H}_2\text{O}}$ from the hydrothermal system. Currently, direct fluid exchange between the lake and
341 the underlying magmatic-hydrothermal system appears limited (van Hinsberg et al., 2017), but
342 fluids from the hydrothermal system do flow out at the lowermost springs with only a small
343 crater lake seepage contribution (Palmer, 2009). The $\delta^{18}\text{O}$ composition of these lowermost
344 seepage waters is significantly lighter at 0.5‰ compared to the approximately 8‰ $\delta^{18}\text{O}$ of the
345 lake water (Palmer, 2009). With the present dataset, we cannot differentiate between these
346 possibilities.

347

348 **Implications**

349 We analyzed the $\delta^{18}\text{O}$ composition of the crystalline water and sulfate group of gypsum from
350 Kawah Ijen crater lake, and determined the fractionation factors between gypsum and fluid for
351 these components. Gypsum preferentially incorporates isotopically heavy water $\delta^{18}\text{O}$, in
352 agreement with previous studies, but has a small preference for light sulfate group $\delta^{18}\text{O}$. Using
353 these fractionation factors to reconstruct the $\delta^{18}\text{O}$ of gypsum formation fluids from 1817 to 2008
354 shows a shift from positive, heavy isotopic compositions recorded by the current lake water and
355 gypsum formed during passive degassing to a lighter composition for the 1817 phreato-magmatic
356 eruption. We attribute this difference to either a shorter-lived and smaller lake prior to the 1817
357 eruption, or a lake with a more direct connection to its underlying magmatic-hydrothermal
358 system. These aspects could not be determined from the gypsum elemental record, showing the
359 value of a combined elemental and isotopic approach. The oxygen-isotopic record from gypsum
360 can thus provide insights into the state of the Kawah Ijen system in the past, and can similarly be
361 applied to other environments where gypsum precipitates from a fluid.

362

363 **Acknowledgments**

364
365 We thank William Mark and Richard Heemskerk (University of Waterloo) for their assistance
366 with $\delta^{18}\text{O}$ analyses of spring water and gypsum samples. We also thank Corentin Caudron, Maria
367 Martínez-Cruz and the other participants of the Cities on Volcanoes 8 Wet Volcanoes workshop
368 for discussion on the Kawah Ijen system. We acknowledge funding from the McGill University
369 Graduate Mobility Award, Mineralogical Association of Canada Travel Grant, and the Cities on
370 Volcanoes 8 Travel Grant to SBU, and the Canadian National Science and Engineering Research
371 Council (NSERC) and le Fonds Québécois de la Recherche sur la Nature et les Technologies
372 (FQRNT) to VvH and BG. We thank Dmitri Rouwet and an anonymous reviewer for the
373 insightful comments that improved the manuscript,.

374 **References**

- 375
376 Africano, F. and Bernard, A. (2000). Acid alteration in the fumarolic environment of Usu volcano,
377 Hokkaido, Japan. *Journal of Volcanology and Geothermal Research*, 97(1-4), 475-495.
378
379 Anonymous “Oudgast” (1820), Mengelingen, *Bataviaasche Courant*. (In Dutch).
380
381 Blaak, C (1920) *Het klimaat van den Idjen*. Koninklijke Natuurkundige Vereeniging Monografie
382 V. Kolff & Co. Batavia, Weltevreden (In Dutch).
383
384 Bosch, C.J. (1858). *Uitbarstingen der vulkanen Idjin en Raun (Banjoewangi)*. *Tijdschrift voor*
385 *Indische Taal-, Land- en Volkenkunde*, 7, 265–286 (In Dutch).
386
387 Caudron, C., Syahbana, D. K., Lecocq, T., van Hinsberg, V., McCausland, W., Triantafyllou, A.,
388 Camelbeeck, T., Bernard, A., and Suroño (2015). Kawah Ijen volcanic activity: a review.
389 *Bulletin of volcanology*, 77(3), 1-39.
390
391 Caudron, C., Champion, R., Rouwet, D., Lecocq, T., Capaccioni, B., Syahbana, D., Purwanto, B.H.,
392 and Bernard, A. (2017). Stratification at the Earth's largest hyperacidic lake and its
393 consequences. *Earth and Planetary Science Letters*, 459, 28-35.
394
395 Delmelle, P. and Bernard, A. (1994). Geochemistry, mineralogy, and chemical modeling of the
396 acid crater lake of Kawah Ijen Volcano, Indonesia. *Geochimica et cosmochimica acta*,
397 58(11), 2445-2460.

- 398
399 Delmelle, P. and Bernard, A. (2000). Downstream composition changes of acidic volcanic waters
400 discharged into the Banyupahit stream, Ijen caldera, Indonesia. *Journal of Volcanology and*
401 *Geothermal Research*, 97(1-4), pp.55-75.
402
403 Delmelle, P., Bernard, A., Kusakabe, M., Fischer, T. P., and Takano, B. (2000). Geochemistry of
404 the magmatic–hydrothermal system of Kawah Ijen volcano, East Java, Indonesia. *Journal*
405 *of Volcanology and Geothermal Research*. 97(1). 31-53.
406
407 Delmelle P., Bernard A. (2015) The Remarkable Chemistry of Sulfur in Hyper-Acid Crater Lakes:
408 A Scientific Tribute to Bokuichiro Takano and Minoru Kusakabe. In: Rouwet D.,
409 Christenson B., Tassi F., Vandemeulebrouck J. (eds) *Volcanic Lakes. Advances in*
410 *Volcanology*. Springer, Berlin, Heidelberg.
411
412 Fulignati, P., Gioncada, A., Sbrana, A. (1998). Geologic model of the magmatic-hydrothermal
413 system of Vulcano (Aeolian Island Italy). *Mineralogy and Petrology*. 62, 195–222.
414
415 Gázquez, F., Evans, N.P., and Hodell, D.A. (2017). Precise and accurate isotope fractionation
416 factors ($\alpha^{17}\text{O}$, $\alpha^{18}\text{O}$ and α^{D}) for water and $\text{CaSO}_4 \cdot 2\text{H}_2\text{O}$ (gypsum). *Geochimica et*
417 *Cosmochimica Acta*, 198, pp.259-270.
418
419 Gonfiantini, R. and Fontes, J.C. (1963). Oxygen isotopic fractionation in the water of
420 crystallization of gypsum. *Nature*, 200.
421
422 Google Earth 6.0. (2015). Kawah Ijen volcano 8°03'28.08"S, 114°14'30.73"E, elevation 0.. 3D
423 map. Eye al. 3.42 km. viewed 7 July 2019.<<http://www.google.com/earth/index.html>>.
424
425 Gunawan, H., Caudron, C., Pallister, J., Primulyana, S., Christenson, B., Mccausland, W., Van
426 Hinsberg, V., Lewicki, J., Rouwet, D., Kelly, P. and Kern, C., and others. (2017). New
427 insights into Kawah Ijen's volcanic system from the wet volcano workshop experiment.
428 *Geological Society, London, Special Publications*, 437, pp.SP437-7.
429
430 Handley, H.K., Macpherson, C.G., Davidson, J.P., Berlo, K. & Lowry, D. (2007). Constraining
431 fluid and sediment contributions to subduction-related mag- matism in Indonesia: Ijen
432 Volcanic Complex. *Journal of Petrology*, 48. 1155–1183.
433
434 Hurst T., Hasimoto, T., Terada, A. (2015) Crater lake energy and mass balance in Rouwet, D.,
435 Christenson, B.W., Tassi, F., Vandemeulebrouck, J. (eds) *Volcanic Lakes*, Springer:
436 Heidelberg.
437
438 Junghuhn, F. (1853). *Java: Deszelfs Gedaante, Bekleding en Inwendige Structuur.*, 3, 14th and
439 15th Sketches. P.N. van Kampen, Amsterdam. 976–1047. (In Dutch)
440
441 Leschenault de la Tour, J. (1805). Notice sur un lac d'acide sulfurique qui se trouve au fond d'un
442 volcan du Mont-Idienne, situe dans la province de Bagnia-Vangni, côte de l'île de Java.
443 *Am. Musm Hist. Nat* 18. 425-446. (In French).

- 444
445 Lewicki, J.L., Caudron, C., van Hinsberg, V.J., and Hilley, G.E. (2016). High spatio-temporal
446 resolution observations of crater lake temperatures at Kawah Ijen volcano, East Java,
447 Indonesia. *Bulletin of Volcanology*, 78(8). 53.
448
- 449 Lloyd, R.M. (1968). Oxygen isotope behavior in the sulfate-water system. *Journal of Geophysical*
450 *Research*, 73(18). 6099-6110.
451
- 452 Löhr, A.J., Sluik, R., Olaveson, M.M., Ivorra, N., Van Gestel, C.A., and Van Straalen, N.M.
453 (2006). Macroinvertebrate and algal communities in an extremely acidic river and the
454 Kawah Ijen crater lake (pH < 0.3), Indonesia. *Archiv für Hydrobiologie*, 165(1). 1-21.
455
- 456 Luhr, J. F., Carmichael, I. S., and Varekamp, J. C. (1984). The 1982 eruptions of El Chichón
457 Volcano, Chiapas, Mexico: mineralogy and petrology of the anhydrite bearing pumices.
458 *Journal of Volcanology and Geothermal Research*, 23(1). 69-108.
459
- 460 Kemmerling, G.L.L. (1921). *Het Idjen Hoogland. De geologie en geomorphologie van den Idjen.*
461 *Koninklijke Natuurkundige Vereniging Monografie II, G. Kolff & Co, Weltevreden-*
462 *Batavia.*
463
- 464 Kusakabe, M., Komoda, Y., Takano, B., and Abiko, T. (2000). Sulfur isotopic effects in the
465 disproportionation reaction of sulfur dioxide in hydrothermal fluids: implications for the
466 $\delta^{34}\text{S}$ variations of dissolved bisulfate and elemental sulfur from active crater lakes. *Journal*
467 *of Volcanology and Geothermal Research*, 97(1-4), 287-307.
468
- 469 Mather, T.A., McCabe, J.R., Rai, V.K., Thiemens, M.H., Pyle, D.M., Heaton, T.H.E., Sloane, H.J.
470 and Fern, G.R. (2006). Oxygen and sulfur isotopic composition of volcanic sulfate aerosol
471 at the point of emission. *Journal of Geophysical Research: Atmospheres*, 111(D18).
472
- 473 Martínez M., Fernández E., Valdés J., Barboza V., van der Laat R., Duarte E., Malavassi E.,
474 Sandoval L., Barquero J., and Marino T. (2000) Chemical evolution and volcanic activity
475 of the active crater lake of Poás Volcano, Costa Rica, 1993–1997. *Journal of Volcanology*
476 *and Geothermal Research* 97. 127–141
477
- 478 Müller, I.A., Brunner, B., Breuer, C., Coleman, M., and Bach, W. (2013a). The oxygen isotope
479 equilibrium fractionation between sulfite species and water. *Geochimica Cosmochimica*
480 *Acta* 120, 562–581.
481
- 482 Müller, I.A., Brunner, B., and Coleman, M. (2013b). Isotopic evidence of the pivotal role of sulfite
483 oxidation in shaping the oxygen isotope signature of sulfate. *Chemical Geology*. 354, 186–
484 202.
485
- 486 Palmer, S.C.J (2009). Hydrogeochemistry of the upper Banyu Pahit River valley, Kawah Ijen
487 volcano, Indonesia. 106 p. MSc thesis. McGill University, Montreal, Canada.
488

- 489 Palmer, S.C., van Hinsberg, V.J., McKenzie, J.M., and Yee, S. (2011). Characterization of acid
490 river dilution and associated trace element behavior through hydrogeochemical modeling:
491 A case study of the Banyu Pahit River in East Java, Indonesia. *Applied Geochemistry*,
492 26(11).1802-1810.
493
- 494 Rodríguez, A., van Bergen, M.J., and Eggenkamp, H.G.M., (2018) Experimental evaporation of
495 hyperacid brines: Effects on chemical composition and chlorine isotope fractionation.
496 *Geochimica et Cosmochimica Acta* 222, 467-484.
497
- 498 Rouwet D., and Ohba T. (2015) Isotope Fractionation and HCl Partitioning During Evaporative
499 Degassing from Active Crater Lakes. In: Rouwet D., Christenson B., Tassi F.,
500 Vandemeulebrouck J. (eds) *Volcanic Lakes. Advances in Volcanology*. Springer, Berlin,
501 Heidelberg
502
- 503 Rouwet D., and Tassi F. (2011) Geochemical monitoring of volcanic lakes. A generalized box
504 model for active crater lakes. *Annals of Geophysics* 54 161-173.
505
- 506 Rowe, G.L. Jr. (1994). Oxygen, hydrogen, and sulfur isotope systematics of the crater lake system
507 of Poás Volcano, Costa Rica. *Geochemical Journal* 28(3). 26-287.
508
- 509 Rye R.O., and Stoffregen R.E. (1995) Jarosite-water oxygen and hydrogen isotope fractionations:
510 preliminary experimental data. *Economic Geology* 90. 2336-2342
511
- 512 Schmidt, G.A. (1999): Forward modeling of carbonate proxy data from planktonic foraminifera
513 using oxygen isotope tracers in a global ocean model. *Paleoceanography*, 14. 482-497
514
- 515 Seal, R.R, Alpers, C.N., and Rye, R.O. (2000). Stable isotope systematics of sulfate minerals.
516 *Reviews in Mineralogy and Geochemistry*, 40 (1). 541-602.
517
- 518 Stoffregen R.E., Rye R.O., and Wasserman M.D. (1994) Experimental studies of alunite: 1. ^{18}O -
519 ^{16}O and D-H fractionation factors between alunite and water at 250-450°C. *Geochimica*
520 *Cosmochimica Acta*, 58. 903-916
521
- 522 Swanson, S.E., and Kearney, C.S. (2008). Anhydrite in the 1989–1990 lavas and xenoliths from
523 Redoubt Volcano, Alaska. *Journal of Volcanology and Geothermal Research*, 175(4), 509-
524 516.
525
- 526 Takano, B., Suzuki, K., Sugimori, K., Ohba, T., Fazlullin, S.M., Bernard, A., Sumarti, S., Sukhyar,
527 R., and Hirabayashi, M. (2004). Bathymetric and geochemical investigation of Kawah Ijen
528 crater lake, East Java, Indonesia. *Journal of Volcanology and Geothermal Research*,
529 135(4), 299-329.
530
- 531 Truesdell A. H. (1974) Oxygen isotope activities and concentrations in aqueous salt solutions at
532 elevated temperatures: Consequences for isotope geochemistry. *Earth and Planetary*
533 *Science Letters* 23, 387- 396
534

- 535 Utami, S.B., van Hinsberg, V.J., Ghaleb, B., and Pinti, D.L. (2019). Growth-zoned gypsum
536 stalactite from the Kawah Ijen volcanic lake, Indonesia, records a > 40-year record of
537 volcanic activity. *Bulletin of Volcanology*, 81(9):52.
538
- 539 van Hinsberg V.J., and Williams-Jones A.E. (2008) Using mineral-fluid element partitioning to
540 reconstruct crater lake fluid chemistry at Kawah Ijen volcano, Indonesia. IAVCEI
541 conference, Reykjavik, Iceland
542
- 543 van Hinsberg, V.J., Berlo, K., Sumarti, S., van Bergen, M.J., and Williams-Jones, A.E. (2010).
544 Extreme alteration by hyperacidic brines at Kawah Ijen volcano, East Java, Indonesia: II.
545 Metasomatic imprint and element fluxes. *Journal of Volcanology and Geothermal
546 Research*, 196, 169–184.
547
- 548 van Hinsberg, V.J., Vigouroux, N., Palmer, S.J., Berlo, K., Scher, S., Mauri, G., Williams-Jones,
549 A.E., McKenzie, J., Williams-Jones, G., and Fischer, T. (2017) Element flux to the
550 environment of the passively degassing Kawah Ijen volcano, Indonesia, and implications
551 for estimates of the global volcanic flux. *Special Issue on Volcanic Lakes*, Geological
552 Society London.
553
- 554 van Stempvoort, D.R., and Krouse, H.R. Controls of $\delta^{18}\text{O}$ in sulfate: Review of experimental
555 data and application to specific environments in C.N. Alpers, and D.W. Blowes, (Eds)
556 (1994.) *Environmental Geochemistry of Sulfide Oxidation*. Washington (D.C.): ACS
557 Symposium Series; American Chemical Society. 446-480
558
- 559 Varekamp, J.C., and Kreulen, R. (2000). The stable isotope geochemistry of volcanic lakes, with
560 examples from Indonesia. *Journal of Volcanology and Geothermal Research* 97(1), 309-
561 327.
562
- 563 Zeebe, R.E. (2010). A new value for the stable oxygen isotope fractionation between dissolved
564 sulfate ion and water. *Geochimica et Cosmochimica Acta*, 74(3), 818-828.
565

566 List of Figure Captions

567 **Figure 1:** Panoramic view of the Kawah Ijen volcanic lake area, adapted from a Google Earth
568 image (Google Earth, 2015). The white box indicates the location of the gypsum plateau and
569 upper springs as well as the fall deposit. (a) Gypsum cemented tephra fall deposit above the
570 gypsum plateau, (b) Cascading gypsum plateau, c) Gypsum stalactite tips with spring water
571 dripping from them.
572

573 **Figure 2:** Conceptual model of formation and isotopic exchange for a Kawah Ijen gypsum
574 stalactite. The gypsum stalactite tip and surface are continuously coated by a film of the parent
575 fluid (PF), which in this case is the crater lake seepage water. Gypsum precipitates by cooling of
576 this fluid and its evaporation, resulting in rapid growth of a transparent tip and slower concentric
577 growth outward. The continuous contact between the stalactite and water ensures uninterrupted
578 growth. Determination of the isotopic compositions for parental fluids ($\delta^{18}\text{O}_{\text{fluid}}^{\text{H}_2\text{O}}$ and

579 $\delta^{18}\text{O}_{\text{gypsum}}^{\text{SO}_4}$) and gypsum ($\delta^{18}\text{O}_{\text{gypsum}}^{\text{H}_2\text{O}}$ and $\delta^{18}\text{O}_{\text{gypsum}}^{\text{SO}_4}$) allows for the fractionation factors for
580 α_{water} and α_{sulfate} to be determined, as well as to calculate the $\alpha(\text{SO}_4\text{-H}_2\text{O})_{\text{fluid}}$, which is a measure
581 of the oxygen isotopic equilibrium state of the fluid. Applying the α_{water} and α_{sulfate} to internal
582 zones of the stalactite allows a timeseries of $\delta^{18}\text{O}_{\text{fluid}}^{\text{H}_2\text{O}}$ and $\delta^{18}\text{O}_{\text{gypsum}}^{\text{SO}_4}$ to be reconstructed.

583
584 **Figure 3:** $\delta^{18}\text{O}_{\text{gypsum}}^{\text{H}_2\text{O}}$ and $\delta^{18}\text{O}_{\text{gypsum}}^{\text{SO}_4}$ of Ijen's various gypsum samples, comprising the 1817
585 gypsum cement ('Cement'), the 2009 growth-zoned stalactite tip ('Stalactite'), 2015 spring water
586 ('Water'), and 2009 growth zoned gypsum stalactite ('Zone').

587
588 **Figure 4:** Timeseries of $\delta^{18}\text{O}_{\text{fluid}}^{\text{H}_2\text{O}}$ and $\delta^{18}\text{O}_{\text{fluid}}^{\text{SO}_4}$ for Ijen seepage waters compared to the
589 elemental record reconstructed from gypsum (data from Utami et al., 2019). Solid symbols are
590 for direct measurements, open symbols for reconstructed values. Crater lake, fumarole and
591 groundwater $\delta^{18}\text{O}$ values are shown for reference (from Delmelle et al., 2000; Palmer 2009; van
592 Hinsberg et al., 2017). The orange lines represent periods of volcanic unrest.

593
594 **Supplementary Figure S1:** Isotopic composition (a) and absolute $\delta^{18}\text{O}$ deviation (b) from the
595 certified value (dashed line) for three in-house standards measured at different water volumes
596 (symbols). The measured and corrected $\delta^{18}\text{O}$ of crystalline water extracted from variable
597 amounts of gypsum sample KV09-505 are also shown. (c) A 2nd polynomial fit surface to the
598 measured deviations in $\delta^{18}\text{O}$ as a function of sample $\delta^{18}\text{O}$, showing minimal deviation at the
599 positive $\delta^{18}\text{O}$ values of the gypsum crystalline water.

600

601 List of tables

602 Table 1: $\delta^{18}\text{O}$ compositions of gypsum stalactite zones, brine and gypsum cement from the 1817
603 fall deposit. The volume of crystalline water for each gypsum sample, and the age for the growth
604 zones are also listed. All values are relative to V-SMOW/V-SLAP. Uncertainties are the 1
605 standard deviation analytical uncertainty, or uncertainty on the mean.

606 Table 2: Gypsum-water $\delta^{18}\text{O}$ fractionation factors for water and sulfate group, and water-sulfate
607 group fractionation factors for water samples. The temperatures of equilibration based on the
608 water-sulfate fractionation curve of Zeebe (2010) are also listed. Water-sulfate fractionation
609 factors by Gonfiantini and Fontes (1963) and Gazquez et al. (2017) are listed for comparison.

610 Table 3: Reconstructed $\delta^{18}\text{O}$ values for gypsum formation waters ($\delta^{18}\text{O}_{\text{fluid}}^{\text{H}_2\text{O}}$ and $\delta^{18}\text{O}_{\text{fluid}}^{\text{SO}_4}$) and
611 their H₂O-SO₄ fractionation factors. The temperatures of equilibration based on the H₂O-SO₄
612 fractionation curve of Zeebe (2010) are also listed.

Table 1.

Sample Type	Sample ID	Comment	μL	$\delta^{18}\text{O}_{\text{H}_2\text{O}}$	1 s	$\delta^{18}\text{O}_{\text{SO}_4}$
Gypsum stalactite	KV09-505	tip	62	9.4	0.5	
		2009	152	9.6	0.5	
			48	9.5	0.5	
			56	9.7	0.5	
		<i>mean</i>		9.6	0.1	20.9
Gypsum stalactite	KV09-501	zone A-B	61	9.3	0.5	
		1980				22.7
						23.1
		<i>mean</i>		9.3	0.5	22.9
		zone B-C	42	8.9	0.5	
		1991				23.0
						23.1
<i>mean</i>		8.9	0.5	23.0		
Gypsum cement	KS14-001	zone D	89	9.8	0.5	
		2008				22.5
						22.1
		<i>mean</i>		9.8	0.5	22.3
Gypsum cement	KS14-001	1817	59	4.3	0.5	
						17.3
						16.8
<i>mean</i>		4.3	0.5	17.1		
Seepage water	KV15-006			6.67	0.2	
				7.16	0.2	
		<i>mean</i>		6.9	0.3	23.4
					23.3	
					23.3	

1 s

0.3

0.3

0.3

0.3

0.3

0.3

0.3

0.1

0.3

0.3

0.3

0.3

0.3

0.4

0.4

0.4

0.1

Table 2.

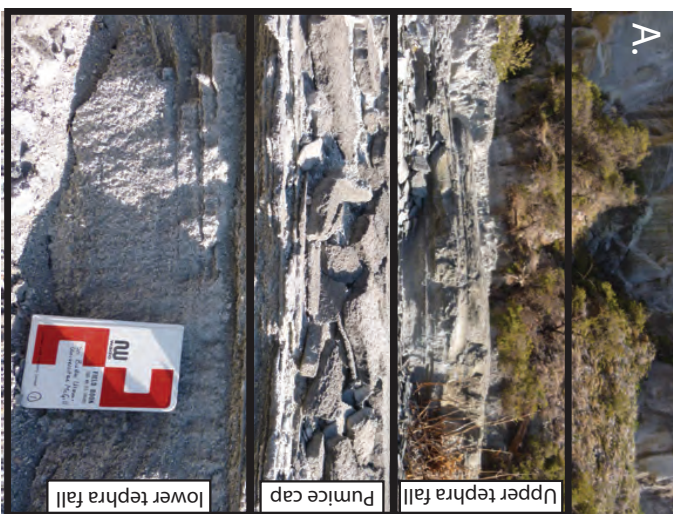
Set	Sample Type	Sample ID	Comment	$\delta^{18}\text{O}_{\text{H}_2\text{O}}$	1 s
1	gypsum stalactite	KV09-505	tip	9.6	0.1
1	seepage water	KV15-006		6.9	0.3
2	gypsum stalactite	KV09-501	zone D	9.8	0.5
2	seepage water	KV15-006		6.9	0.3
3	gypsum stalactite	KV09-501	zone B-C	8.9	0.5
3	seepage water	BP96 2-5	Delmelle and Bernard 2000	6	3
	fractionation factor gypsum / water		set 1	1.0026	0.0003
			set 2	1.0029	0.0006
			set 3	1.0025	0.0029
			mean	1.0027	0.0002
			Gonfiantini and Fontes, 1963	1.0037	0.0005
			Gazquez et al. 2017	1.0035	0.0002

$\delta^{18}\text{O}_{\text{SO}_4}$	1 s	$\alpha \text{ SO}_4/\text{H}_2\text{O}$	Equilibration T (Zeebe 2010)
20.9	0.3		
23.3	0.1	1.016	$64 \pm 2 \text{ }^\circ\text{C}$
22.3	0.3		
23.3	0.1	1.016	$64 \pm 2 \text{ }^\circ\text{C}$
23.0	0.1		
22.5	0.2	1.016	$65 \pm 21 \text{ }^\circ\text{C}$
0.9976	0.0003		
0.9990	0.0003		
1.0005	0.0002		
0.9990	0.0014		

Table 3

Sample Type	Sample ID	Comment	Year	$\delta^{18}\text{O}_{\text{H}_2\text{O}}$	1 s	$\delta^{18}\text{O}_{\text{SO}_4}$	1 s
Gypsum stalactite	KV09-501	zone A-B	1980	6.6	0.4	23.9	0.3
		zone B-C	1991	6.2	0.3	24.0	0.1
		zone D	2008	7.1	0.4	23.3	0.3
Gypsum cement	KS14-001		1817	1.6	0.2	18.1	0.4

α SO ₄ /H ₂ O	Equilibration T (Zeebe 2010)
1.017	58 ± 3 °C
1.018	54 ± 3 °C
1.016	65 ± 4 °C
1.016	63 ± 3 °C



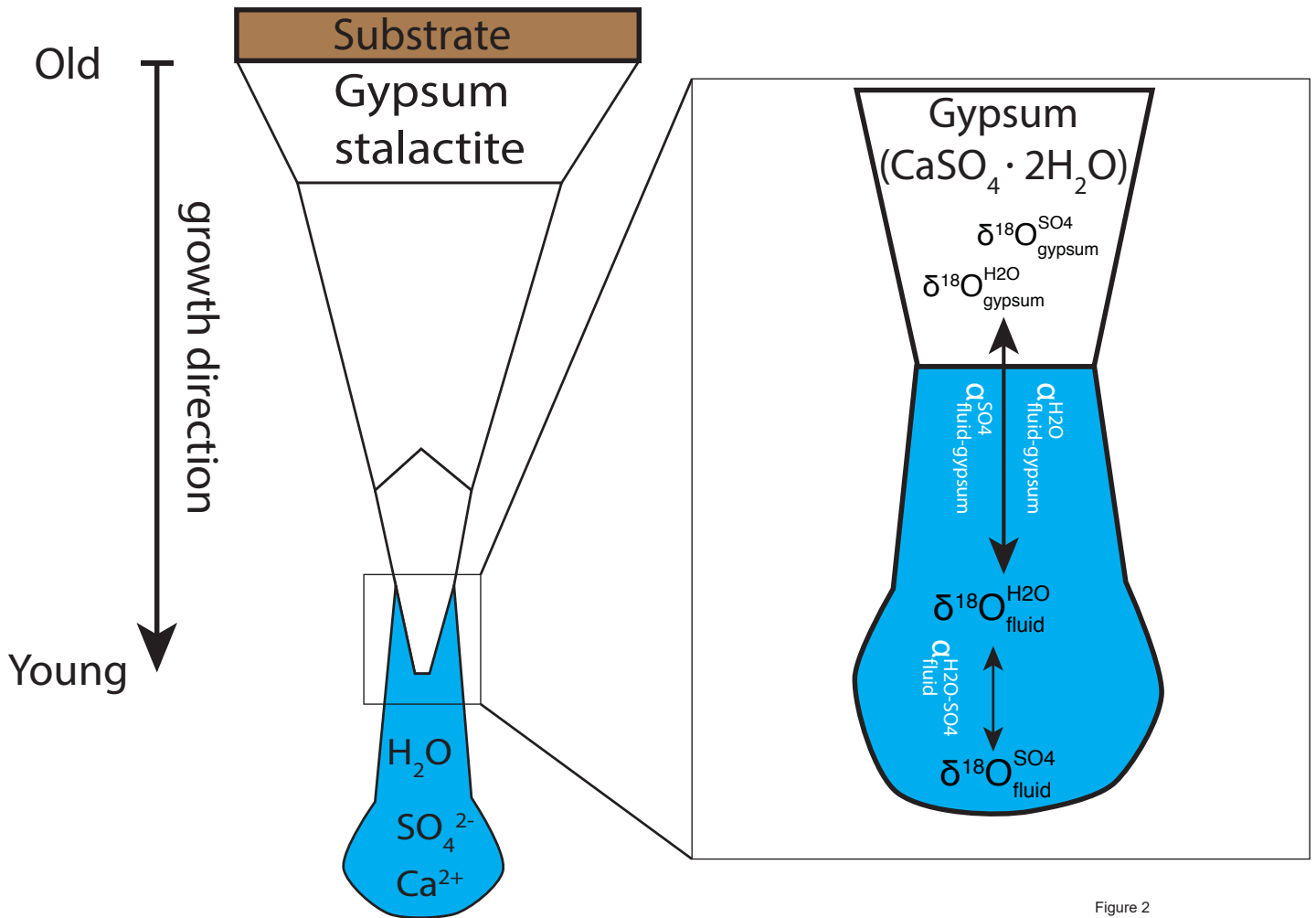


Figure 2

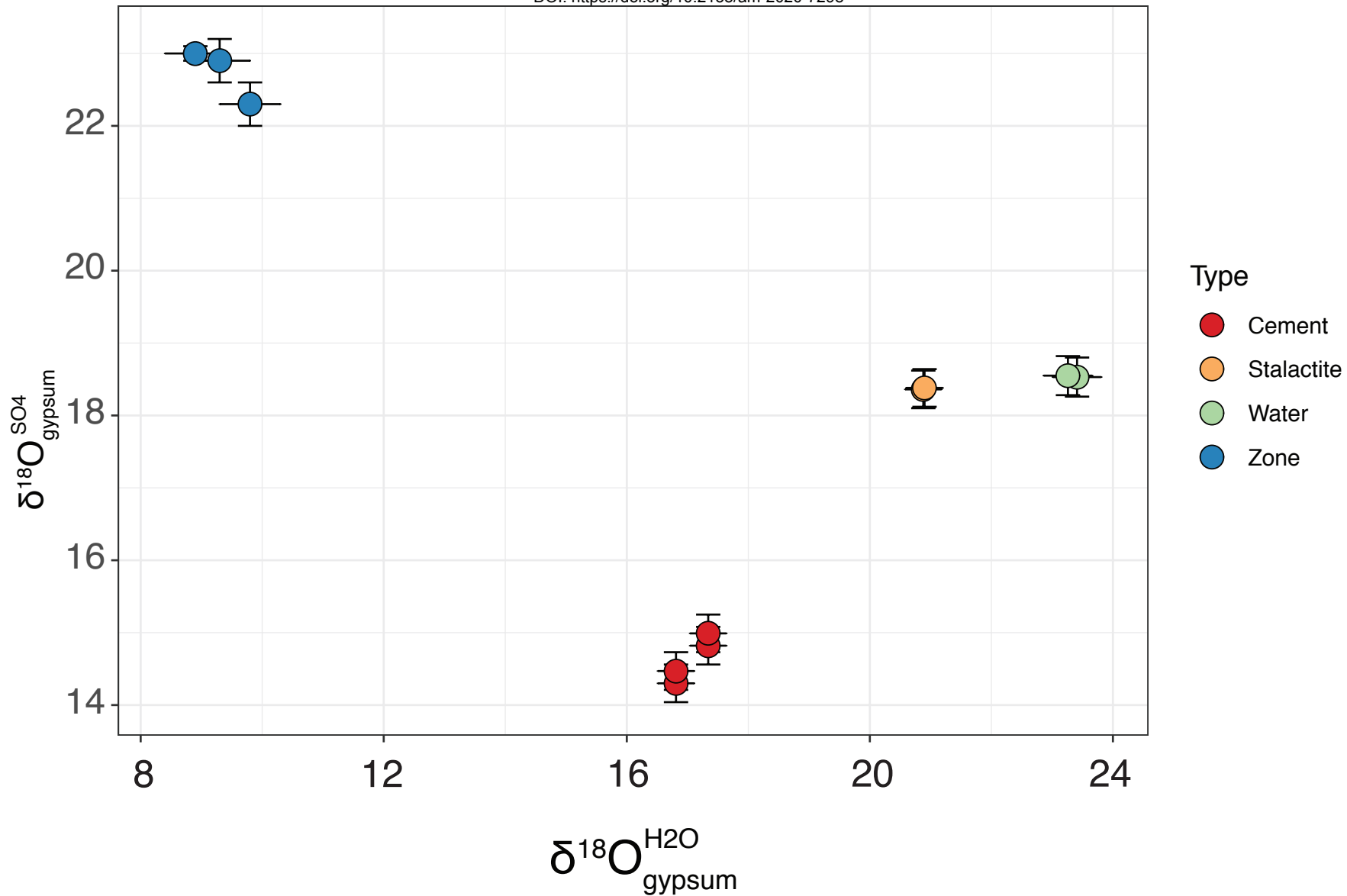


Figure 4

